Published for SISSA by Springer
Received: January 10, 2023
Revised: August 11, 2023
Accepted: October 17, 2023
Published: October 25, 2023

Probing the electroweak symmetry breaking history with gravitational waves

Zizhuo Zhao,[a,b] **Yuefeng Di,**[c,d] **Ligong Bian**[e,f] **and Rong-Gen Cai**[g,c,k]

[a] *University of Chinese Academy of Sciences (UCAS), Beijing 100049, P.R. China*
[b] *International Center for Theoretical Physics Asia-Pacific, Beijing/Hangzhou, P.R. China*
[c] *CAS Key Laboratory of Theoretical Physics, Institute of Theoretical Physics, Chinese Academy of Sciences, Beijing 100190, P.R. China*
[d] *School of Physical Sciences, University of Chinese Academy of Sciences, No. 19A Yuquan Road, Beijing 100049, P.R. China*
[e] *Department of Physics and Chongqing Key Laboratory for Strongly Coupled Physics, Chongqing University, Chongqing 401331, P.R. China*
[f] *Center for High Energy Physics, Peking University, Beijing 100871, P.R. China*
[g] *School of Physical Science and Technology, Ningbo University, Ningbo 315211, P.R. China*
[k] *School of Fundamental Physics and Mathematical Sciences, Hangzhou Institute for Advanced Study, University of Chinese Academy of Sciences, Hangzhou 310024, P.R. China*

E-mail: zhaozizhuo23@mails.ucas.ac.cn, diyuefeng22@mails.ucas.ac.cn, lgbycl@cqu.edu.cn, cairg@itp.ac.cn

Abstract: We perform three dimensional lattice simulation of the electroweak symmetry breaking process through two-step vacuum-like phase transitions with one step being first-order. Our results show that: 1) when the electroweak symmetry breaking is driven by the beyond Standard Model theories through the *Higgs-portal*, the gravitational wave spectra produced from the phase transitions are of broken power-law shape; 2) when the electroweak symmetry breaking is induced by a first-order phase transition of a high-scale theory respecting the global U(1) symmetry, cosmic strings can form and then decay through particle radiation. The two scenarios can be distinguished through probing the stochastic gravitational wave backgrounds. Our study suggests that the stochastic gravitational wave backgrounds provide an alternative way to probe the beyond Standard Model theories relevant to the electroweak symmetry breaking in the early Universe.

Keywords: Cosmology of Theories BSM, Phase Transitions in the Early Universe

ArXiv ePrint: 2204.04427

https://doi.org/10.1007/JHEP10(2023)158

JHEP10(2023)158

Contents

1 Introduction

While the phase transition (PT) pattern in the Standard Model (SM) of particle physics is *cross-over* [1], a first-order PT is a general prediction in many new physics models beyond the SM [2, 3]. The first-order PTs can produce stochastic gravitational wave (GW) backgrounds, which are detectable by LIGO and Virgo [4], Laser Interferometer Space Antenna (LISA) [5], Taiji [6], TianQin [7], Big Bang Observer (BBO) [8], and DECi-hertz Interferometer Gravitational wave Observatory (DECIGO) [9], etc. Recently, the constraints on new physics admitting low-scale and high-scale first-order PTs are placed by PPTA [10] (and NANOGraV [11]) and LIGO-Virgo [12, 13]. Therefore, the stochastic GW background searches open a new astronomy window to probe new physics beyond the SM [2, 14, 15].

The Early Universe may settle down to the electroweak vacuum through multi-step phase transitions which is in general motivated by dark matter, electroweak baryogenesis, and gauge hierarchy problem and can be classified as three models. Firstly, the electroweak symmetry breaking (EWSB) process can occur through two-step electroweak PTs with one or two steps being first-order (dubbed as type-a PT), where the Baryon Asymmetry of the Universe can be generated through electroweak baryogenesis [16–26], and the dark matter can be accommodated together with strong GW signals detectable by LISA and other GW detectors [25, 27–31]. Secondly, the EWSB may occur through dimensional transmutation after hidden sectors undergo first-order PT (dubbed as type-b PT) with detectable GWs [32–41], as in many classically conformal theories (CCT) motivated for the gauge hierarchy problem [42–52]. Therein, the hidden sectors may keep in thermal equilibrium with the SM in the early Universe. Thirdly, when the beyond SM theories that trigger the EWSB obey a global U(1) symmetry (dubbed as type-c PT), cosmic strings can form during the spontaneous symmetry breaking of the U(1) symmetry [53, 54]. When the global U(1) symmetry is the Peccei-Quinn (PQ) symmetry [55–58], the global strings can intimately connected with strong CP problem [59–66] and the axion dark matter physics [3, 67–71]. It

JHEP10(2023)158

was proposed that axion-like models can be probed by LIGO when the PQ symmetry is broken down by a first-order PT associated with GWs production [12, 55–58].

Previous lattice simulations of the GWs produced during the first-order PT process usually adopt a single scalar field to study one-step PT [72–79]. In this paper, we numerically study the dynamical EWSB driven by the above three classes of two-step PTs in the early Universe, and investigate the feature of associated stochastic GW backgrounds. For this purpose, we perform three-dimensional lattice simulation of first-order PT considering dynamics of Higgs and a beyond SM scalar. To the best of our knowledge, the three-dimensional lattice simulation of first-order PT with two scalars haven't been studied before. We study the produced GW spectra of three types of two-step phase transitions with the first- or second-step being first-order PT. We also investigate the formation and evolution of cosmic strings during the first-order PT within a global U(1) theory.

2 Phase transition models

We first introduce three classes of PT models for the study of dynamical EWSB and GWs production. For the type-a PT model, we consider the first-step being a second-order ("2nd") PT and the second-step being a first-order ("1st") one. Since the first-step second-order PT is known to yield null GWs,[1] we focus on the second step first-order PT. The barrier triggering this kind of PT is dominated by the tree-level potential [81], we therefore adopt the thermal effective potential as

$$V_a(\phi,h,T) = \frac{1}{2}(\mu_\phi^2 + c_\phi T^2)\phi^2 + \frac{1}{2}\lambda_{h\phi}h^2\phi^2 + \frac{1}{4}\lambda_\phi\phi^4 + \frac{1}{2}(-\mu_h^2 + c_h T^2)h^2 + \frac{1}{4}\lambda_h h^4\,, \tag{2.1}$$

with $c_\phi = \lambda_\phi/4 + \lambda_{h\phi}/3\,, c_h = (2m_W^2 + m_Z^2 + 2m_t^2)/(4v^2) + \lambda_h/2 + \lambda_{h\phi}/12$. Here, $m_{W,Z,t}$ are masses of $W(Z)$ bosons and top quark, respectively, v (λ_h) is VEV (quartic coupling) of the SM Higgs and are all fixed by the SM precision measurement. In this model, we consider the dark sector can keep in thermal equilibrium with the SM through a moderate Higgs coupling $\lambda_{h\phi} \sim \mathcal{O}(10^{-1})$ which is constrained by the requirement of the PT pattern [28, 81, 82]: the type-a PT occurs with the vacuum transiting from the dark vacuum ($(0, \langle\phi\rangle)$) to the electroweak vacuum ($(\langle h\rangle, 0)$) (the left plot of figure 1). The finial vacuum structure of ($(\langle h\rangle = v, \langle\phi\rangle = 0)$) ensures that there is no mixing between the SM Higgs and the ϕ, and is therefore denoted as "nightmare" scenario for colliders in literatures [81, 83].

For the type-b PT, the barrier driving the first-order PT mostly comes from the Coleman-Weinberg potential, the thermal effective potential contribution from CCT can take the form [84],[2]

$$V_{\rm cct}(\phi,T) = A\phi^4(\log[|\phi|/v_\phi] - 1/4) + BT^2|\phi|^2\,, \tag{2.2}$$

[1] Recently, ref. [80] studied the possibility that the domain wall formed in the first-step second-order PT would affect the second-step first-order PT and the produced GW.

[2] The potential barriers that drive the first-order phase transition come from the tree-level potential (loop-level potential) for type-a PT (type-b and type-c PTs). For the potential barrier coming from the thermal corrections, though our idea still applies, one needs to systematically incorporate thermal contributions to the thermal effective potential [85–90].

JHEP10(2023)158

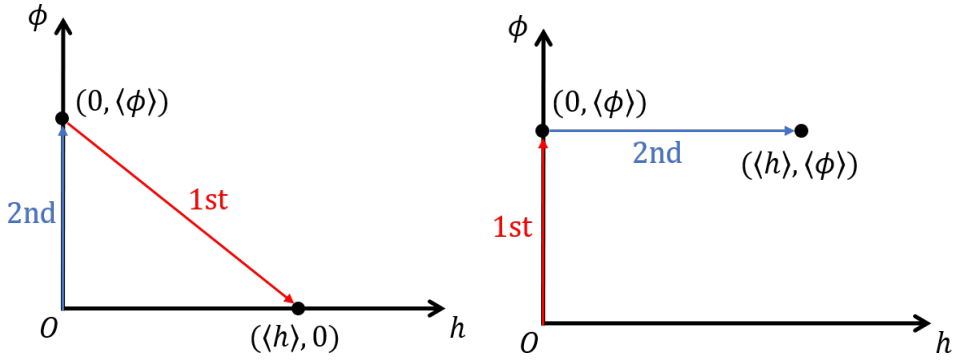

Figure 1. PT patterns for type-a (left), type-b and type-c classes (right).

and the relevant thermal potential for dynamical dimensional transmutation process is

$$V_{\rm dt}(\phi, h, T) = \frac{1}{2}c_h' T^2 h^2 + \frac{1}{4}\lambda_h h^4 - \frac{\lambda_{h\phi}}{4} h^2\phi^2\,, \tag{2.3}$$

with $c_h' = (2m_W^2 + m_Z^2 + 2m_t^2)/(4v^2) + \lambda_h/2 + \lambda_{h\phi}/24$. After the first-step first-order PT occurs in the CCT ($(0,0) \to (0, \langle\phi\rangle)$) with the production of GWs, the vacuum transits from the symmetric phase to CCT's vacuum, the last term of eq. (2.3) triggers the EWSB through the dimensional transmutation process. More exactly, in the second-step PT we have ($(0, \langle\phi\rangle) \to (\langle h\rangle, \langle\phi\rangle)$) where ($\langle h\rangle = \sqrt{(\lambda_{h\phi}\eta^2 - 2c_h' T^2)/(2\lambda_h)}$) when $\lambda_{h\phi}\eta^2 - 2c_h' T^2 > 0$. The parameters A, B characterize the contribution of underlying theories, and the Higgs-portal coupling $\lambda_{h\phi}$ controls the splitting between the electroweak scale and the high-scale CCT.

We consider the PT pattern of the type-c to be similar as type-b, with the vacuum transiting from the symmetric phase to the U(1) vacuum, and then to the electroweak vacuum as shown in the right plot of figure 1.[3] We study the GWs associated with the formation and decay of global strings during this PT. Here, we take the same thermal potential form as in eqs. (2.2), (2.3) with the real scalar ϕ replaced by a complex scalar (Φ) persevering a global U(1) symmetry, i.e., it is the field content of the theory which distinguishes the type-b PT from the type-c PT.

In the simulations of all three types of PTs, we perform the study with (and without) the cosmic expansion effect. The equations of motion for the real scalar fields are taken as:

$$\phi_i'' - \nabla^2\phi_i + 2\mathcal{H}\phi_i' + a^2\frac{dV}{d\phi_i} = 0, \tag{2.4}$$

for the case with cosmic expansion, Here, $\mathcal{H} = a'/a$ is the conformal Hubble parameter and is related with the usual Hubble parameter as $\mathcal{H} = aH$. And, one have

$$\phi_i'' - \nabla^2\phi_i + \frac{dV}{d\phi_i} = 0, \tag{2.5}$$

when the cosmic expansion effect is discarded as in the literatures. The thermal potential V being given above and the $\mathcal{H}$ is the conformal Hubble parameter. $\phi_i = h, \phi$ for type-a

[3]Global cosmic strings might be formed [53] during the process. For early studies on the cosmic defects that might be formed due to "geodesic rule" when vacuum bubbles collide with each other, see refs. [91–100].

JHEP10(2023)158

and type-b PTs, for type-c PT we include also the equation of motion for the Higgs field except for that of the complex scalar Φ with $\phi_i = h, \phi_{1,2}$. At the beginning, we have the initial conditions $\phi_i = \dot{\phi}_i = 0$. When the PT happens, we consider that bubbles simultaneously nucleate in the symmetric phase. The evolution of radiation energy density is considered by following refs. [101, 102] for the case with cosmic expansion, where the energy transfer from vacuum energy to the radiation energy occurs as the PT proceeds. We have vacuum bubbles nucleated with the bubble profile being determined through bounce solutions conducted by *Anybubble* [103] and *FindBounce* [104]. The initial bubble radius (R_0) and the thickness of the critical bubble wall (L_w) can be obtained after match the bubble profile obtained through the bounce solutions with the bubble profiles described by the thin-wall approximation. The thin-wall approximation applies well when the potential barrier is much larger than the vacuum energy, or the true vacuum and the false vacuum are almost degenerate.

For type-a PT, the bubble profiles for the second-step first-order PT in the thin-wall approximation are [105, 106],

$$h(t=0,r) = \eta_h/2\left[1-\tanh\left(\frac{r-R_0}{L_w}\right)\right], \tag{2.6}$$

$$\phi(t=0,r) = \eta_\phi/2\left[1+\tanh\left(\frac{r-R_0}{L_w}\right)\right]. \tag{2.7}$$

Here, $\eta_{h,\phi}$ are vacuum expectation values (VEVs) of dark vacuum and electroweak vacuum when PT occurs. For the type-b PT, the bubble profiles in the thin-wall approximation admit the form of $\phi(t=0,r) = \eta_\phi/2\,[1-\tanh(r-R_0)/L_w]$ with η_ϕ being the VEV of ϕ when the CCT vacuum bubbles nucleate, and $\langle h\rangle = \sqrt{(\lambda_p\eta^2 - 2c_h'T^2)/(2\lambda_h)}$ inside these bubbles. For type-c PT, we take the two real scalar fields of U(1), $\Phi = (\phi_1, \phi_2)$, $\phi_1 = \phi(t=0,\boldsymbol{r})\cos\theta/2$ and $\phi_2 = \phi(t=0,\boldsymbol{r})\sin\theta/2$ where the phase θ is uniformly distributed in the range of $[0, 2\pi]$ with θ being the random phase of the nucleated CCT's vacuum bubbles.

3 GWs production

We calculate GWs by including all scalar contributions involved in PTs and the evolution process of cosmic strings, including bubble collisions and scalar oscillations during the dynamical EWSB process.[4] The equation of motion of tensor perturbations h_{ij} reads [110]

$$\ddot{h}_{ij} - \nabla^2 h_{ij} = 16\pi G T_{ij}^{\rm TT} \tag{3.1}$$

for the case without considering the cosmic expansion. And, we have

$$h_{ij}'' - \partial_k\partial_k h_{ij} + 2\mathcal{H}h_{ij}' - 2(2\mathcal{H}' + \mathcal{H}^2)h_{ij} = 16\pi G T_{ij}^{\rm TT}\,, \tag{3.2}$$

in the conformal time when the cosmic expansion is considered. Here, the superscript TT denotes the transverse-traceless projection. We include both two scalar field contributions

[4] Here we mention that the conventional adopted envelope approximation is still under debate, see refs. [52, 77, 78, 107–109].

JHEP10(2023)158

in the energy-momentum tensor

$$T_{\mu\nu} = \partial_\mu \phi_i \partial_\nu \phi_i - g_{\mu\nu} \frac{1}{2} (\partial \phi_i)^2 \,, \tag{3.3}$$

for type-a and type-b PTs, and

$$T_{\mu\nu} = \partial_\mu \Phi^\dagger \partial_\nu \Phi - g_{\mu\nu} \frac{1}{2} \mathrm{Re}[(\partial_\mathrm{i} \Phi^\dagger \partial^\mathrm{i} \Phi)] \,, \tag{3.4}$$

for type-c PT. When the spontaneous symmetry breaking scale of the global U(1) theory is close to the electroweak scale, one needs to include the contributions to metric perturbations from the Higgs field. And the Higgs gradients would be much smaller and whose contribution is negligible for the case under study where the two scales are separated far away from each other. We evolve equation of motions in eqs. (2.4), (2.5) and tensor perturbations in eqs. (3.1), (3.2) with a code based on *pystella* [111].[5] The energy spectrum of GWs is the GW energy density fraction per logarithmic frequency interval,

$$\Omega_{\mathrm{GW}} = \frac{1}{\rho_c} \frac{d\rho_{\mathrm{GW}}(k)}{d \ln k}, \quad \rho_{\mathrm{GW}}(k) = \frac{1}{32\pi G} \langle \dot{h}_{ij} \dot{h}^{ij} \rangle. \tag{3.5}$$

4 Numerical results

Our simulations are performed on a cubic lattice with the resolution $L^3 = 256^3 \Delta x$, the lattice volume is chosen as $LH = 8$ with H being the Hubble parameter. The time spacing is chosen to be $\Delta t = \Delta x/5$ for type-a(and b) PTs, and $\Delta t = \Delta x/10$ for type-c PT considering better resolution of cosmic strings. The mean bubble separation is obtained as $R_\star = (L^3/N_b)^{1/3}$ with N_b being the number of the generated bubbles during the PT processes, which determines the Lorentz factor for bubbles as $\gamma_\star = R_\star/(2R_0)$, and the wall width as $L_w^\star = L_w/\gamma_\star$ when bubbles collide with each other.

We first study how the EWSB occurs through the three types of two-step PTs. For type-a PT, we consider "nightmare" scenario of the future colliders [83] by adopting $\lambda_{h\phi} = 0.7$ (and $m_\phi = 170\,\mathrm{GeV}$), $\lambda_\phi = 1$ for the benchmark point (BP-1). For type-b PT and type-c PT as illustrated in the right plot of figure 1, we simulate the different phase transition strength of supercooling cases by taking model parameters as: $A = 0.125, B = 0.0095$ (BP-2 and BP-3),[6] with the coupling of $\lambda_{h\phi}$ will be specified later. The bubble parameters (initial bubble radius and initial bubble wall thickness), PT parameters (the PT strengths and the bubble nucleation rates) for the three types of PTs under study are specified in table 1. The bubble nucleation rates are directly connected with the mean bubble separation, see refs. [73, 77, 78, 112]. Here, we use w/o to specify the cases *with/without* cosmic expansion. The values on the left (right) of each column, i.e., before(after) the slash, indicate that cases with (without) cosmic expansion. For the case *with* cosmic expansion, we perform simulations with comoving (conformal) time and space lattices. Since all the parameters of $R_\star(R_0)$, $L_w^\star(L_w)$ are in units of Δx, we observe the values of $R_\star/\Delta x$ and $L_w^\star/\Delta x$ are

[5] https://github.com/zachjweiner/pystella.

[6] For the PQ symmetry breaking through first-order PT, these parameters can be obtained with proper parameter choice as in refs. [55, 58].

JHEP10(2023)158

Benchmark points	BP-1 w/o expansion	BP-2 w/o expansion	BP-3 w/o expansion
$R_0/\Delta x$	13	12	12
$L_w/\Delta x$	6	7	7
$R_\star/\Delta x$	47.06/46.77	46.12/46.67	47.06/45.59
$L_w^\star/\Delta x$	3.31/3.33	3.64/3.59	3.57 /3.68
N_b	161/164	171/175	161/177
PT strength (α)	13.47	28.52	34.67

Table 1. Bubble parameters, and PT strength for three BPs with/without cosmic expansion.

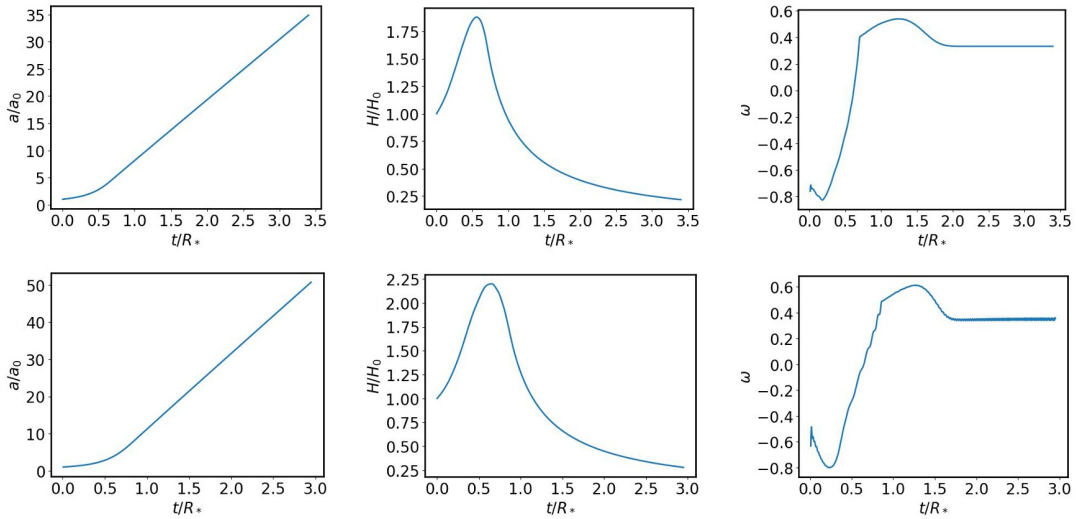

Figure 2. This figure represents the scale factor (left), Hubble parameter (middle), and equation of state (right) for the scenarios of the type-a and type-b PTs with cosmic expansion. The upper plots indicate the scenario of the type-a PT, and the lower plots present the case of type-b PT which is the same as the type-c PT.

similar for both the cases of with and without cosmic expansion. The bubble wall width $L_w^\star/\Delta x$ (when then bubbles are collided with each other) ensures that we have enough lattice spacing resolution.

For the cases with cosmic expansion, we present the corresponding evolution of the normalized scale factor, Hubble parameter, and the equation of state (EoS) for type-a and type-b PTs in figure 2, the type-c PT occurs in the same background as type-b PT. Our simulation indicate that all the three types PT under study occurs in a vacuum-like Universe with EoS being $\omega \sim -0.7$. With the proceeding of the PTs, the evolution of the scale factor finally admit a radiation-dominated FLRW universe with $\omega \approx 1/3$. The rapid changes of the Hubble parameter and EoS reflect the process of the vacuum bubbles collision.

As shown in the figure 3, during the type-a PT process, the decrease of ϕ and the accompanying increase of h indicate that the EWSB occurs with the vacuum transition as $(0, \langle\phi\rangle) \to (\langle h\rangle, 0)$ (see the left plot of figure 1). The EWSB process occurs through

JHEP10(2023)158

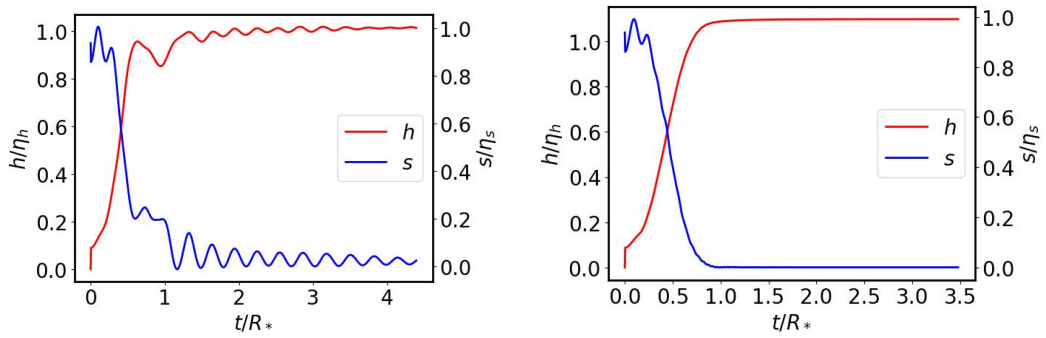

Figure 3. This figure represents a comparison of the mean field values with and without cosmic expansion for the type-a PT. The left plot indicates the scenario of the type-a PT without considering the cosmic expansion, which occurs with the decrease of ϕ and increase of h accompanied with large oscillations of the scalar fields; and the right plot indicates the first-order PT of type-a with cosmic expansion.

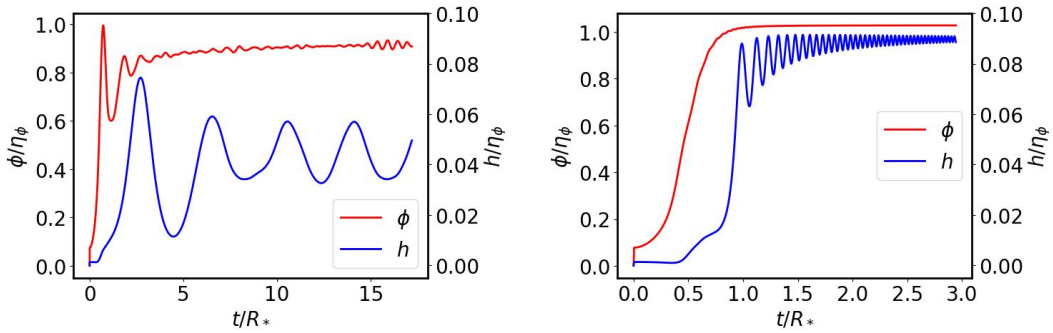

Figure 4. This figure presents the mean field evolutions during the PT processes for type-b PT without (left panel) and with cosmic expansion(right panel). The left (right) panels show that after the ϕ grows to around $\phi/\eta_\phi \sim 0.9(1)$ through a first-order PT the type-b PT complete with $h/\eta_\phi \sim 0.04(0.09)$.

electroweak bubble expansions and merging with each other when the dark vacuum continues to shrink, see figure 8 in appendix A for illustration. When the expansion of the Universe are included, the magnitude of the scalar fields' oscillation appears much smaller.

In the left and right plots of figure 4, we take $\lambda_{h\phi} = 0.002$ to show the dynamical EWSB triggered by TeV scale theories through type-b PT. The feature is the same for much smaller $\lambda_{h\phi}$ where the scale of the beyond SM theories is much higher. The two plots show that the field ϕ quickly gets VEV when the CCT's vacuum bubbles expand and merge with each other. Then, the vacuum transits from the symmetric phase to the CCT's vacuum since the first-step PT is of first-order. Meanwhile, the second-step PT starts as the h gradually increases during the first step PT, where the space distributions of the Higgs field values inherit the same shape as CCT's vacuum bubbles (see top panels of figure 9 in the appendix A). After the first-order PT in CCT, the second step PT process continues and completes, which is slightly slow in comparison with first-order PT. In this way, the EWSB occurs through dimensional transmutation process. During the whole PT process,

JHEP10(2023)158

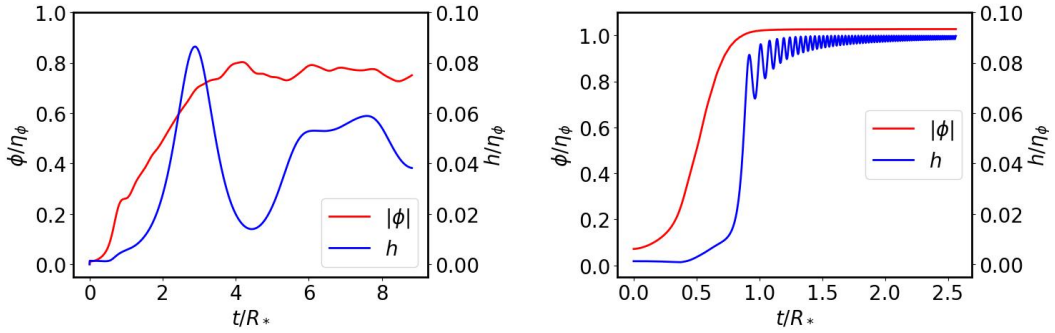

Figure 5. This figure presents the mean field evolutions during the PT processes for type-c PT without (left panel) and with cosmic expansion(right panel). Both the two comments of the complex scalar get VEVs during the PT, and the Higgs field get VEV gradually.

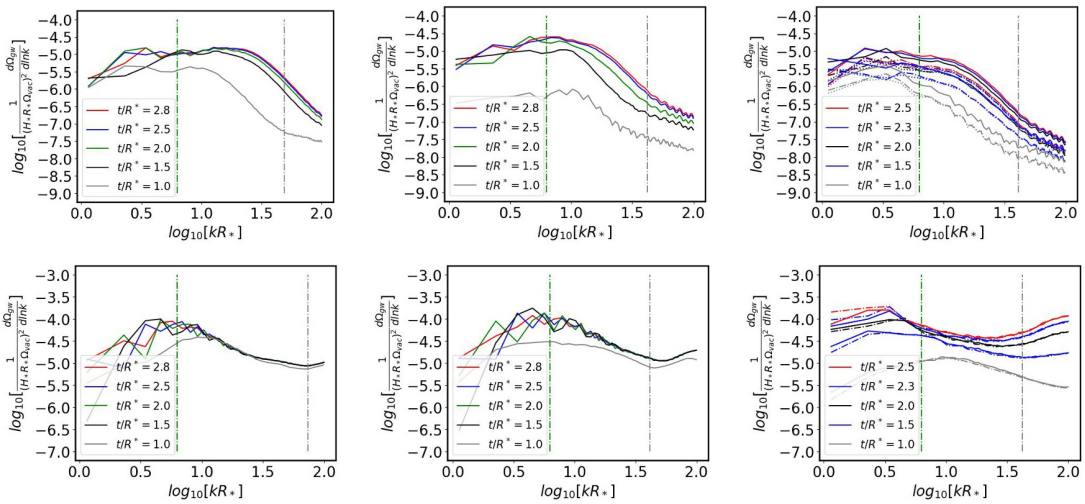

Figure 6. Normalized GWs spectra for three type PTs, with upper(and lower) panels present the scenarios without (and with) expansion of the Universe. The left two plots are the case of type-a PT, the middle and right two plots are the cases of type-b and type-c PTs. For the type-c PT, the GWs from energy-momentum tensor of real and imaginary fields are depicted by dash-dot and dotted curves, and the solid curves indicate the sum of the two contributions. The positions of $R_\star$ and L_w are marked with green and grey dash-dot vertical lines.

the dynamics of the inherited bubbles is totally different from the one of the CCT's vacuum bubbles. In the figure 5, we present the type-c PT scenario. Both the two components of the complex scalar Φ (ϕ_1 and ϕ_2) get VEV during CCT's vacuum bubbles nucleation, expansion, and percolation process. The behavior of $|\phi| = \sqrt{\phi_1^2 + \phi_2^2}$ is almost the same as ϕ in the type-b PT as shown in figure 4. During the PT process, EWSB occurs when the Higgs field gets VEV through dimensional transmutation as type-b. We find that the cosmic strings form after the CCT's bubbles collide and disappear with the proceeds of the phase transition (see figure 10 and figure 11 in appendix A for details).

We now turn to study the property of the GWs spectra generated from the PT processes of the three types. In figure 6, the GWs spectra at five different moments during these PTs

JHEP10(2023)158

are plotted for illustration. Here, $\Omega_{\rm vac} = \Delta\rho/\rho_c$ with $\Delta\rho$ being the latent heat released by the PT and $H_\star$ is the Hubble parameter at the end time of our simulations. The results show that GW spectra for all three PTs are all of broken power-law shape. For the scenario of type-a PT, the contributions from h and ϕ are comparable, and the top-left plot shows two peak frequencies located roughly corresponding to the mean bubble separation $R_\star$ and the wall width L_w, respectively. In the high-frequency range, the scalar oscillations in the true vacuum yield the second peak of the GW spectrum. When the two peak frequencies are separated clearly as shown in the benchmark, the numerical simulation results suggest that we can have two peak frequencies rather than one as previous found in refs. [113, 114]. When the PT's scale is close to the Planck scale, the contribution from the high-frequency range (the second peak) should be taken into account. The contribution from the CCT's bubble dynamics dominates the GWs production in the type-b and type-c PTs, the contribution from the Higgs field is negligible since the EWSB proceeds through a second-order PT. Note that the poor resolution in the IR region with $kR_\star < 10$ is due to the limitation of the lattice volume, which is supposed to approach to the causality limit [115]. We numerically confirmed that the GW spectra in the high-frequency range depends on the lattice spacing, which is consistent with observations obtained in refs. [77, 78]. We note that, the simulations resemble vacuum transitions rather than the thermal transitions one might expect from a transition in the electroweak sector. Here, the Higgs field is expected to couple to other light fields, creating friction and heating the primordial plasma. Meanwhile, we include the energy evolution from the false vacuum to the radiation for the case with the cosmic expansion. For the current study, due to the limitation of computational resources, we focus on the study of the GW spectra around the peak frequency corresponding to $R_\star$ generated by the bubbles collision and discard the UV region on the right hand side of L_w which suffer from numerical artifacts.

With these simulation results at hand, we can fit the GW spectra for the case with cosmic expansion that is absent in literatures. We take the following function,

$$\Omega_{\rm gw} = \tilde{\Omega}(k_p)\frac{(a+b)^c k_p^b k^a}{\left(b k_p^{(a+b)/c} + a k^{(a+b)/c}\right)^c}\,, \tag{4.1}$$

for the low-frequency peak broken power-law spectra predicted by the tree type PTs. Here, $\tilde{\Omega}(k_{p1}) \propto (\alpha/(1+\alpha))^2 (H_\star/\beta)^2$ is the amplitude of the GW spectrum at the peak frequency ($k = 2\pi/R_\star$) corresponding to the mean bubble separation ($R_\star = (8\pi)^{1/3} v_w/\beta$). The fitted parameters are shown in table 2. These parameters of a, b, c are fitted by averaged the magnitudes of the GW spectra in the low-frequency range. These results lead to different GW spectrum between type-a and type-b PTs for the same β, α and T_*. We further note that, with the bulk flow approximation, the GW spectrum can be much shallower (steeper) in the IR region (and UV region) [107]. For the simultaneous nucleation, ref. [78] shows that the power-law in the UV region can depend on the specific potential shape. The contribution to GWs from the dynamics of the Higgs during the PT is negligible for both type-b and type-c PTs under study.

Now, we are going to investigate the detectable PTs with the PT scales far smaller than the Planck scale, where we do not consider the GW contributions locating at high

JHEP10(2023)158

Benchmark points	BP-1	BP-2	BP-3
a	2.35	1.71	0.58
b	0.97	1.58	1.16
c	0.08	1.08	0.01

Table 2. Fitted parameters of GW spectra for six benchmark points.

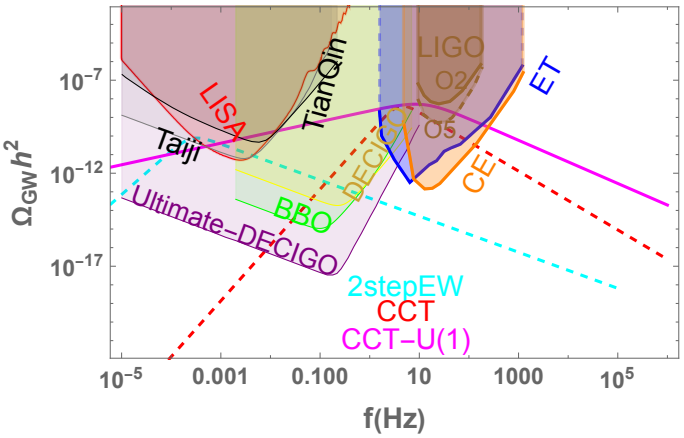

Figure 7. The spectra of GWs of type-a (2stepEW, cyan curve) with $\alpha = 0.24, \beta/H_\star = 20, T_\star = 100\,\text{GeV}$, type-b (CCT, red curve) and type-c (CCT-U (1), magenta curve) PTs with $\alpha = 11, \beta/H_\star = 50, T_\star = 10^6\,\text{GeV}$.

frequency's peak. For the spectrum of the GWs production in type-a and type-b PTs, we parameterize the GW spectrum as the form in ref. [77]

$$h^2\Omega(f) = h^2\tilde{\Omega}(f_p)\frac{(a+b)^c f_p^b f^a}{(b f_p^{(a+b)/c} + a f^{(a+b)/c})^c}\,, \tag{4.2}$$

with the low frequency peak locating at $f_p = 1.6\times10^{-5}/(\beta R_\star)(\beta/H_\star)(T_\star/100)(g_\star/100)^{1/6}$ Hz (with $R_\star \approx (8\pi)^{1/3}v_w/\beta$), and the magnitude of the GW spectrum being $\tilde{\Omega}(f_p) = 1.67\times10^{-5}(100/g_\star(T_\star))^{1/3}(\alpha/(1+\alpha))^2(H_\star/\beta)^2$ at present. With the a, b, c in the eq. (4.2) being obtained above, we can obtain the GW spectra for the PT's parameter: β, α, $T_\star$ being predicted by beyond SM theories. For the type-c PT, the GW spectrum is of a more gradual shape, and we have cosmic strings formation and decay during the PT process (see figure 11 of appendix A for cosmic strings evolution). In figure 7, we show the spectra of GW's in the type-a PT, type-b and type-c PTs with $\lambda_{h\phi} \sim \mathcal{O}(10^{-8})$.

5 Conclusions and discussions

In this paper, we study three types of two-step EWSB generally predicted by some beyond SM theories. Our observations show that GW observations can help to differentiate different classes of beyond SM physics. We find that, when the underlying theory with (without) a global U(1) symmetry inducing the EWSB through a first-order PT, the produced GW

JHEP10(2023)158

spectrum is of broken power-law shape. The GWs produced during the type-a PT can be probed by LISA, TianQin, and Taiji since the PT is triggered by the beyond SM sector of electroweak scale. The GWs produced during PeV scale type-b and type-c PTs fall into the sensitivity regions of LIGO-Virgo, and the additional global U(1) symmetry makes the GW spectrum from the type-c PT distinguishable from the case of type-b PT. Therefore, this study indicates that GW is complementary to colliders for searching new physics relevant to dark matter and baryogenesis at electroweak scale, and the GW detection provides an alternative approach to probe the new physics at PeV scale which is unaccessible by colliders.

Notice that the previous studies in the literature on GWs from two-step phase transition with one step being first-order (e.g., ref. [26]) are based on the GW spectrum obtained by the lattice simulation of first-order phase transition utilizing a single scalar [73, 75, 76, 113, 116]. Here, our study are based on the lattice simulation of two-step phase transitions with two scalar fields, the cosmic expansion effects are included also.

Acknowledgments

We thank John T. Giblin, Marek Lewicki, Daniel Cutting, David Weir, Adrien Florio, Zach Weiner, Daniel G. Figueroa, Michael J. Ramsey-Musolf, Xue-Feng Zhang, Shao-Jiang Wang, Yue Zhao, Huai-Ke Guo, and Jing Liu for communications and discussions. The work of Ligong Bian is supported by the National Key Research and Development Program of China Grant No. 2021YFC2203004, the National Natural Science Foundation of China under the grants Nos. 12075041, 12147102, 12322505 and the Fundamental Research Funds for the Central Universities of China (No. 2021CDJQY-011 and No. 2020CDJQY-Z003), and Chongqing Natural Science Foundation (Grants No.cstc2020jcyj-msxmX0814). RGC is supported in part by the National Key Research and Development Program of China Grant Nos. 2020YFC22015092 and 2021YFA0718304 and the National Natural Science Foundation of China under the grant Nos. 11821505 and 11991052.

A Numerical details

We present three time slices during the expansion and collision of the nucleated bubbles for the type-a phase transition in figure 8. These plots represent the bubble dynamics when the first-order PT of type-a occurs (see the left plot of the figure 1). We firstly have the electroweak vacuum inside the bubbles which is the false vacuum of ϕ, and region outside vacuum bubbles is the dark vacuum rather than the electroweak vacuum. Latter, bubbles start to collide and merge with each other, where Higgs gets VEV through the electroweak vacuum eating the dark vacuum, With the proceeding of the PT, we further present a later time to show that the transition from the dark vacuum to the electroweak vacuum will complete, and that in most places the normalized value of h (and ϕ) approaches 1 (and 0) (see the right plots). In this way, the EWSB occurs.

In figure 9, the bubble dynamics for the type-b PT are presented. These plots show that when the bubbles of CCT's vacuum nucleate, the distribution of Higgs field value also shares the same bubble shape at the early stage since the Higgs gets VEV through the

JHEP10(2023)158

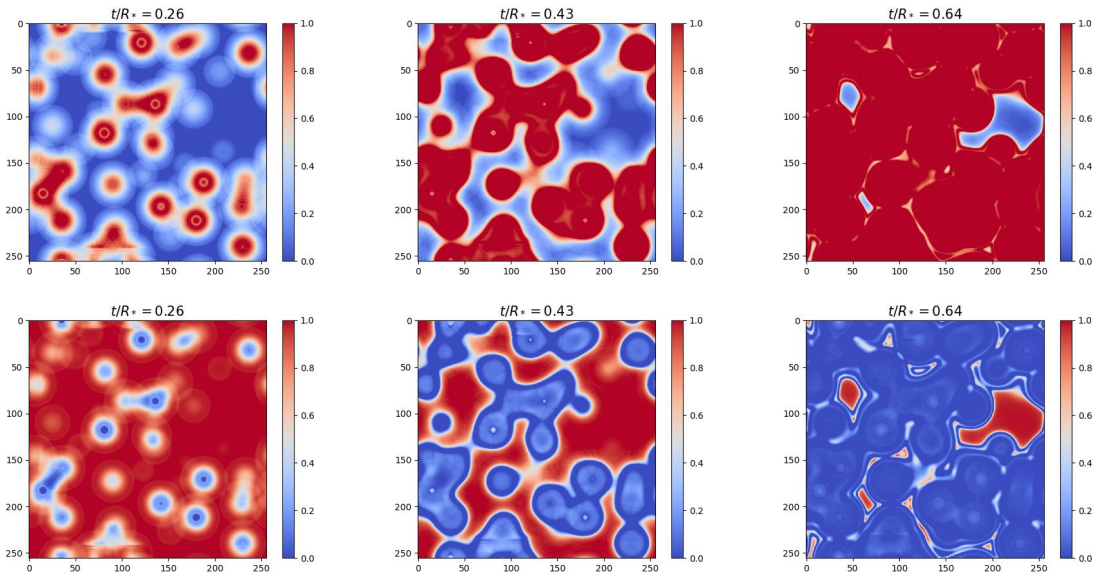

Figure 8. For illustration, we plot the 2d slices for bubble dynamics of ϕ (top plots) and h (bottom plots) at different times during the second-step first-order PT for the type-a PT (with cosmic expansion). The color bar represents the normalized magnitude of h and ϕ at each lattice point.

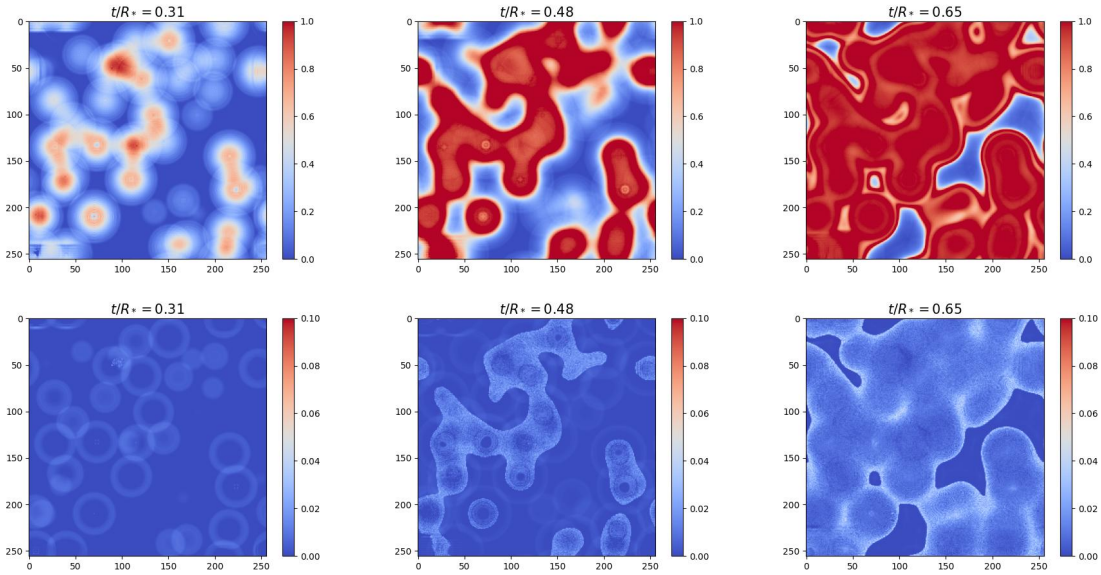

Figure 9. The 2d slices for bubbles dynamic of ϕ (top panels) and Higgs field h (bottom panels) at different time during the type-b PT (with cosmic expansion). Here, the color bar is the same as figure 8.

JHEP10(2023)158

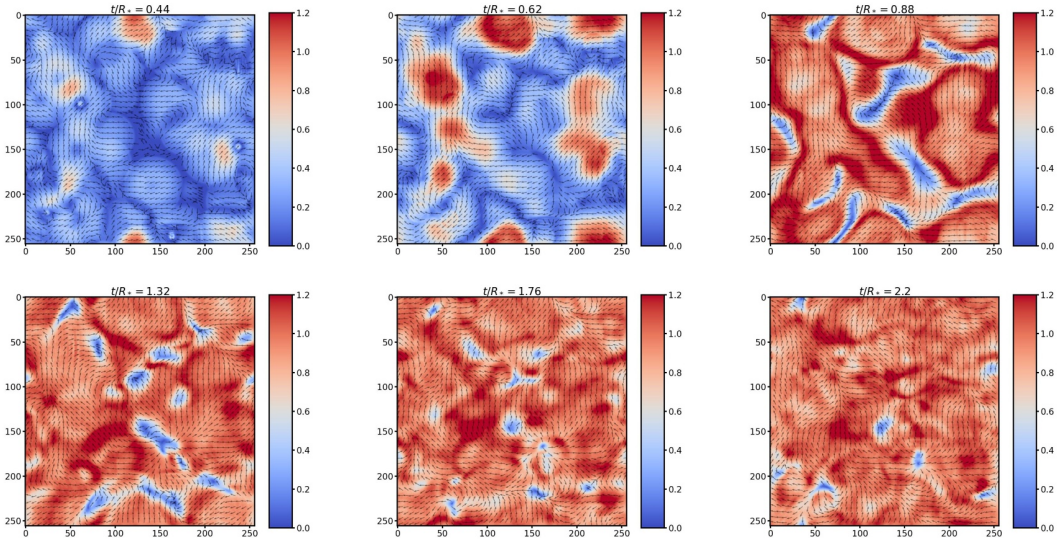

Figure 10. An illustration for the bubble dynamics and phase distribution at different time for the type-c PT without cosmic expansion. The color bar here is to represent the magnitude of the complex field at each lattice point, and the arrows represent the phases at each place.

dimensional transmutation after ϕ gets VEV. In the right plots, one can find that after the vacuum start to fall into the CCT's vacuum (i.e., after the merge of CCT's vacuum bubbles), the EWSB finishes later as can also be found in mean field value evolution shown in the figure 4.

For the first-step of type-c PTs, during the first-order PT process, we find that cosmic strings form after the U(1) vacuum bubbles collide with each other at $t/R_\star > 1$. We present the 2d slices of bubble dynamics and phase variations in figure 10. As shown in the these plots, before the bubbles collide with each other, the phase in each bubble is the same. After the bubbles start to collide with each other, the phases start to redistribute as can be found in the top-right plot. Some time later after $t/R_\star > 1$, we find that the vortex and anti-vortex pairs are formed, where the false vacua are trapped inside the true vacua (see bottom three plots). Here, we present the case without considering cosmic expansion for illustration, and for the case with cosmic expansion we have much quicker formation and disappear of these vortex and anti-vortex feature, and therefore a much quicker evolution of the cosmic strings, this is because that the PT of this case proceeds much faster when the cosmic expansion is considered.

Following the convention of [117], the energy density stored in the cosmic string is given by

$$E = \frac{1}{2}|\partial_t \Phi|^2 + \frac{1}{2}|\nabla \Phi|^2 + V_{\rm cct}(\Phi, T)\,. \tag{A.1}$$

Here, $\Phi \equiv \rho \exp(i\theta)$ with $\rho = \sqrt{\phi_1^2 + \phi_2^2}$ and $\theta = \arcsin\left[\frac{\phi_1}{\sqrt{\phi_1^2+\phi_2^2}}\right]$. We then obtain

$$E \equiv E_\rho + E_\theta, \tag{A.2}$$

JHEP10(2023)158

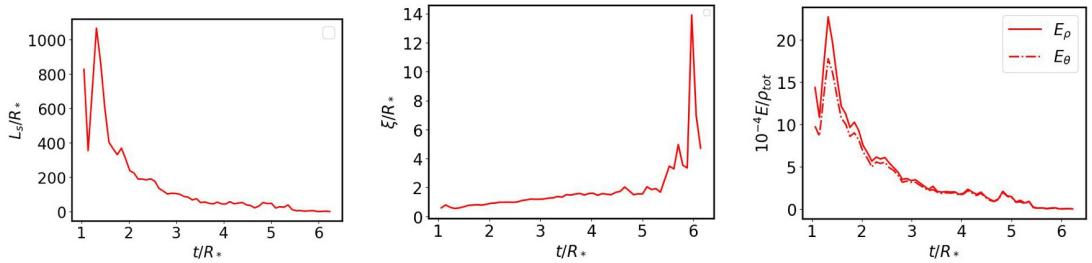

Figure 11. An illustration for the cosmic strings during the type-c PT without cosmic expansion. Left: string length evolutions; middle: the corresponding evolutions of mean string separation; right: the string energy density of E_ρ(solid lines) and E_θ (dash-dot lines).

where the energy density of massive modes (ρ) is

$$E_\rho = \frac{1}{2}(\partial_t \rho)^2 + \frac{1}{2}(\nabla \rho)^2 + V_{\rm cct}(\rho), \tag{A.3}$$

and that of the Goldstone modes (θ) is defined as

$$E_\theta = \frac{\rho^2}{2}\left[(\partial_t \theta)^2 + (\nabla \theta)^2\right]. \tag{A.4}$$

Please note that here this θ is not the phase associated with the nucleated CCT's bubbles.

As shown in figure 11, our simulations indicate that cosmic strings start to form after vacuum bubbles collide with each other, i.e., $t/R_\star > 1$, and disappear depending on the number of bubble and bubble velocities. Here, we take $|\Phi|/\eta_\Phi < 0.1$ to identify cosmic strings. See the *string animation* for details of the dynamical process. Figure 11 demonstrates that the cosmic string length (L_s) decreases (left panel), and the mean string separation (top-middle panel) exponentially increases until cosmic strings disappear. The mean string separation here is defined as V/L_s and its minimum is around $R_\star$ when cosmic strings are formed at the beginning. To illustrate the relation between the bubble dynamics and the radiation mode of cosmic strings, we present the energy density of comic strings (including massive mode and goldstone mode) in the right panel of figure 11. Here, we find that these global strings formed in first-order phase transitions mostly decay to particles, with the energy density of the massive modes is slightly larger than that of the goldstone modes. For the study on particle radiations after a second order phase transition of some U(1) theories, we refer to refs. [117, 118].

JHEP10(2023)158

References

[1] M. D'Onofrio, K. Rummukainen and A. Tranberg, *Sphaleron Rate in the Minimal Standard Model*, *Phys. Rev. Lett.* **113** (2014) 141602 [arXiv:1404.3565] [INSPIRE].

[2] A. Mazumdar and G. White, *Review of cosmic phase transitions: their significance and experimental signatures*, *Rept. Prog. Phys.* **82** (2019) 076901 [arXiv:1811.01948] [INSPIRE].

[3] R. Caldwell et al., *Detection of early-universe gravitational-wave signatures and fundamental physics*, *Gen. Rel. Grav.* **54** (2022) 156 [arXiv:2203.07972] [INSPIRE].

[4] LIGO Scientific and Virgo collaborations, *Observation of Gravitational Waves from a Binary Black Hole Merger*, *Phys. Rev. Lett.* **116** (2016) 061102 [arXiv:1602.03837] [INSPIRE].

[5] LISA collaboration, *Laser Interferometer Space Antenna*, arXiv:1702.00786 [INSPIRE].

[6] W.-H. Ruan, Z.-K. Guo, R.-G. Cai and Y.-Z. Zhang, *Taiji program: Gravitational-wave sources*, *Int. J. Mod. Phys. A* **35** (2020) 2050075 [arXiv:1807.09495] [INSPIRE].

[7] TianQin collaboration, *TianQin: a space-borne gravitational wave detector*, *Class. Quant. Grav.* **33** (2016) 035010 [arXiv:1512.02076] [INSPIRE].

[8] V. Corbin and N.J. Cornish, *Detecting the cosmic gravitational wave background with the big bang observer*, *Class. Quant. Grav.* **23** (2006) 2435 [gr-qc/0512039] [INSPIRE].

[9] K. Yagi and N. Seto, *Detector configuration of DECIGO/BBO and identification of cosmological neutron-star binaries*, *Phys. Rev. D* **83** (2011) 044011 [*Erratum ibid.* **95** (2017) 109901] [arXiv:1101.3940] [INSPIRE].

[10] X. Xue et al., *Constraining Cosmological Phase Transitions with the Parkes Pulsar Timing Array*, *Phys. Rev. Lett.* **127** (2021) 251303 [arXiv:2110.03096] [INSPIRE].

[11] NANOGrav collaboration, *Searching for Gravitational Waves from Cosmological Phase Transitions with the NANOGrav 12.5-Year Dataset*, *Phys. Rev. Lett.* **127** (2021) 251302 [arXiv:2104.13930] [INSPIRE].

[12] A. Romero et al., *Implications for First-Order Cosmological Phase Transitions from the Third LIGO-Virgo Observing Run*, *Phys. Rev. Lett.* **126** (2021) 151301 [arXiv:2102.01714] [INSPIRE].

[13] Y. Jiang and Q.-G. Huang, *Constraining the gravitational-wave spectrum from cosmological first-order phase transitions using data from LIGO-Virgo first three observing runs*, *JCAP* **06** (2023) 053 [arXiv:2203.11781] [INSPIRE].

[14] C. Caprini et al., *Science with the space-based interferometer eLISA. II: Gravitational waves from cosmological phase transitions*, *JCAP* **04** (2016) 001 [arXiv:1512.06239] [INSPIRE].

[15] C. Caprini et al., *Detecting gravitational waves from cosmological phase transitions with LISA: an update*, *JCAP* **03** (2020) 024 [arXiv:1910.13125] [INSPIRE].

[16] V.A. Kuzmin, V.A. Rubakov and M.E. Shaposhnikov, *On the Anomalous Electroweak Baryon Number Nonconservation in the Early Universe*, *Phys. Lett. B* **155** (1985) 36 [INSPIRE].

JHEP10(2023)158

[17] M.E. Shaposhnikov, *Possible Appearance of the Baryon Asymmetry of the Universe in an Electroweak Theory*, *JETP Lett.* **44** (1986) 465 [INSPIRE].

[18] M.E. Shaposhnikov, *Baryon Asymmetry of the Universe in Standard Electroweak Theory*, *Nucl. Phys. B* **287** (1987) 757 [INSPIRE].

[19] D.E. Morrissey and M.J. Ramsey-Musolf, *Electroweak baryogenesis*, *New J. Phys.* **14** (2012) 125003 [arXiv:1206.2942] [INSPIRE].

[20] H.H. Patel and M.J. Ramsey-Musolf, *Stepping Into Electroweak Symmetry Breaking: Phase Transitions and Higgs Phenomenology*, *Phys. Rev. D* **88** (2013) 035013 [arXiv:1212.5652] [INSPIRE].

[21] N. Blinov, J. Kozaczuk, D.E. Morrissey and C. Tamarit, *Electroweak Baryogenesis from Exotic Electroweak Symmetry Breaking*, *Phys. Rev. D* **92** (2015) 035012 [arXiv:1504.05195] [INSPIRE].

[22] S. Inoue, G. Ovanesyan and M.J. Ramsey-Musolf, *Two-Step Electroweak Baryogenesis*, *Phys. Rev. D* **93** (2016) 015013 [arXiv:1508.05404] [INSPIRE].

[23] M.J. Ramsey-Musolf, P. Winslow and G. White, *Color Breaking Baryogenesis*, *Phys. Rev. D* **97** (2018) 123509 [arXiv:1708.07511] [INSPIRE].

[24] K.-P. Xie, L. Bian and Y. Wu, *Electroweak baryogenesis and gravitational waves in a composite Higgs model with high dimensional fermion representations*, *JHEP* **12** (2020) 047 [arXiv:2005.13552] [INSPIRE].

[25] M. Jiang, L. Bian, W. Huang and J. Shu, *Impact of a complex singlet: Electroweak baryogenesis and dark matter*, *Phys. Rev. D* **93** (2016) 065032 [arXiv:1502.07574] [INSPIRE].

[26] A. Beniwal et al., *Gravitational wave, collider and dark matter signals from a scalar singlet electroweak baryogenesis*, *JHEP* **08** (2017) 108 [arXiv:1702.06124] [INSPIRE].

[27] L. Bian and Y.-L. Tang, *Thermally modified sterile neutrino portal dark matter and gravitational waves from phase transition: The Freeze-in case*, *JHEP* **12** (2018) 006 [arXiv:1810.03172] [INSPIRE].

[28] L. Bian and X. Liu, *Two-step strongly first-order electroweak phase transition modified FIMP dark matter, gravitational wave signals, and the neutrino mass*, *Phys. Rev. D* **99** (2019) 055003 [arXiv:1811.03279] [INSPIRE].

[29] M.J. Baker and J. Kopp, *Dark Matter Decay between Phase Transitions at the Weak Scale*, *Phys. Rev. Lett.* **119** (2017) 061801 [arXiv:1608.07578] [INSPIRE].

[30] M.J. Baker, M. Breitbach, J. Kopp and L. Mittnacht, *Dynamic Freeze-In: Impact of Thermal Masses and Cosmological Phase Transitions on Dark Matter Production*, *JHEP* **03** (2018) 114 [arXiv:1712.03962] [INSPIRE].

[31] W. Chao, H.-K. Guo and J. Shu, *Gravitational Wave Signals of Electroweak Phase Transition Triggered by Dark Matter*, *JCAP* **09** (2017) 009 [arXiv:1702.02698] [INSPIRE].

[32] P. Schwaller, *Gravitational Waves from a Dark Phase Transition*, *Phys. Rev. Lett.* **115** (2015) 181101 [arXiv:1504.07263] [INSPIRE].

[33] J. Jaeckel, V.V. Khoze and M. Spannowsky, *Hearing the signal of dark sectors with gravitational wave detectors*, *Phys. Rev. D* **94** (2016) 103519 [arXiv:1602.03901] [INSPIRE].

[34] D. Croon, V. Sanz and G. White, *Model Discrimination in Gravitational Wave spectra from Dark Phase Transitions*, *JHEP* **08** (2018) 203 [arXiv:1806.02332] [INSPIRE].

JHEP10(2023)158

[35] M. Breitbach et al., *Dark, Cold, and Noisy: Constraining Secluded Hidden Sectors with Gravitational Waves*, *JCAP* **07** (2019) 007 [arXiv:1811.11175] [INSPIRE].

[36] M. Fairbairn, E. Hardy and A. Wickens, *Hearing without seeing: gravitational waves from hot and cold hidden sectors*, *JHEP* **07** (2019) 044 [arXiv:1901.11038] [INSPIRE].

[37] I. Baldes, *Gravitational waves from the asymmetric-dark-matter generating phase transition*, *JCAP* **05** (2017) 028 [arXiv:1702.02117] [INSPIRE].

[38] K. Tsumura, M. Yamada and Y. Yamaguchi, *Gravitational wave from dark sector with dark pion*, *JCAP* **07** (2017) 044 [arXiv:1704.00219] [INSPIRE].

[39] M. Aoki, H. Goto and J. Kubo, *Gravitational Waves from Hidden QCD Phase Transition*, *Phys. Rev. D* **96** (2017) 075045 [arXiv:1709.07572] [INSPIRE].

[40] D. Croon and G. White, *Exotic Gravitational Wave Signatures from Simultaneous Phase Transitions*, *JHEP* **05** (2018) 210 [arXiv:1803.05438] [INSPIRE].

[41] I. Baldes and C. Garcia-Cely, *Strong gravitational radiation from a simple dark matter model*, *JHEP* **05** (2019) 190 [arXiv:1809.01198] [INSPIRE].

[42] R. Foot, A. Kobakhidze, K.L. McDonald and R.R. Volkas, *A Solution to the hierarchy problem from an almost decoupled hidden sector within a classically scale invariant theory*, *Phys. Rev. D* **77** (2008) 035006 [arXiv:0709.2750] [INSPIRE].

[43] S. Iso, N. Okada and Y. Orikasa, *The minimal B-L model naturally realized at TeV scale*, *Phys. Rev. D* **80** (2009) 115007 [arXiv:0909.0128] [INSPIRE].

[44] C. Englert, J. Jaeckel, V.V. Khoze and M. Spannowsky, *Emergence of the Electroweak Scale through the Higgs Portal*, *JHEP* **04** (2013) 060 [arXiv:1301.4224] [INSPIRE].

[45] A. Farzinnia, H.-J. He and J. Ren, *Natural Electroweak Symmetry Breaking from Scale Invariant Higgs Mechanism*, *Phys. Lett. B* **727** (2013) 141 [arXiv:1308.0295] [INSPIRE].

[46] T. Hur and P. Ko, *Scale invariant extension of the standard model with strongly interacting hidden sector*, *Phys. Rev. Lett.* **106** (2011) 141802 [arXiv:1103.2571] [INSPIRE].

[47] W.-F. Chang, J.N. Ng and J.M.S. Wu, *Shadow Higgs from a scale-invariant hidden* $\mathrm{U}(1)_s$ *model*, *Phys. Rev. D* **75** (2007) 115016 [hep-ph/0701254] [INSPIRE].

[48] S. Iso, N. Okada and Y. Orikasa, *Classically conformal B-L extended Standard Model*, *Phys. Lett. B* **676** (2009) 81 [arXiv:0902.4050] [INSPIRE].

[49] R. Jinno and M. Takimoto, *Probing a classically conformal B-L model with gravitational waves*, *Phys. Rev. D* **95** (2017) 015020 [arXiv:1604.05035] [INSPIRE].

[50] L. Marzola, A. Racioppi and V. Vaskonen, *Phase transition and gravitational wave phenomenology of scalar conformal extensions of the Standard Model*, *Eur. Phys. J. C* **77** (2017) 484 [arXiv:1704.01034] [INSPIRE].

[51] S. Iso, P.D. Serpico and K. Shimada, *QCD-Electroweak First-Order Phase Transition in a Supercooled Universe*, *Phys. Rev. Lett.* **119** (2017) 141301 [arXiv:1704.04955] [INSPIRE].

[52] M. Lewicki and V. Vaskonen, *Gravitational wave spectra from strongly supercooled phase transitions*, *Eur. Phys. J. C* **80** (2020) 1003 [arXiv:2007.04967] [INSPIRE].

[53] T.W.B. Kibble, *Topology of Cosmic Domains and Strings*, *J. Phys. A* **9** (1976) 1387 [INSPIRE].

[54] M.B. Hindmarsh and T.W.B. Kibble, *Cosmic strings*, *Rept. Prog. Phys.* **58** (1995) 477 [hep-ph/9411342] [INSPIRE].

JHEP10(2023)158

[55] P.S.B. Dev, F. Ferrer, Y. Zhang and Y. Zhang, *Gravitational Waves from First-Order Phase Transition in a Simple Axion-Like Particle Model*, *JCAP* **11** (2019) 006 [arXiv:1905.00891] [INSPIRE].

[56] B. Von Harling, A. Pomarol, O. Pujolàs and F. Rompineve, *Peccei-Quinn Phase Transition at LIGO*, *JHEP* **04** (2020) 195 [arXiv:1912.07587] [INSPIRE].

[57] A. Ghoshal and A. Salvio, *Gravitational waves from fundamental axion dynamics*, *JHEP* **12** (2020) 049 [arXiv:2007.00005] [INSPIRE].

[58] L. Delle Rose, G. Panico, M. Redi and A. Tesi, *Gravitational Waves from Supercool Axions*, *JHEP* **04** (2020) 025 [arXiv:1912.06139] [INSPIRE].

[59] A. Vilenkin and T. Vachaspati, *Radiation of Goldstone Bosons From Cosmic Strings*, *Phys. Rev. D* **35** (1987) 1138 [INSPIRE].

[60] R.L. Davis, *Cosmic Axions from Cosmic Strings*, *Phys. Lett. B* **180** (1986) 225 [INSPIRE].

[61] D. Harari and P. Sikivie, *On the Evolution of Global Strings in the Early Universe*, *Phys. Lett. B* **195** (1987) 361 [INSPIRE].

[62] C. Hagmann and P. Sikivie, *Computer simulations of the motion and decay of global strings*, *Nucl. Phys. B* **363** (1991) 247 [INSPIRE].

[63] R.A. Battye and E.P.S. Shellard, *Global string radiation*, *Nucl. Phys. B* **423** (1994) 260 [astro-ph/9311017] [INSPIRE].

[64] R.A. Battye and E.P.S. Shellard, *Axion string constraints*, *Phys. Rev. Lett.* **73** (1994) 2954 [astro-ph/9403018] [INSPIRE].

[65] M. Yamaguchi, M. Kawasaki and J. Yokoyama, *Evolution of axionic strings and spectrum of axions radiated from them*, *Phys. Rev. Lett.* **82** (1999) 4578 [hep-ph/9811311] [INSPIRE].

[66] C. Hagmann, S. Chang and P. Sikivie, *Axion radiation from strings*, *Phys. Rev. D* **63** (2001) 125018 [hep-ph/0012361] [INSPIRE].

[67] M. Buschmann, J.W. Foster and B.R. Safdi, *Early-Universe Simulations of the Cosmological Axion*, *Phys. Rev. Lett.* **124** (2020) 161103 [arXiv:1906.00967] [INSPIRE].

[68] M. Gorghetto, E. Hardy and G. Villadoro, *Axions from Strings: the Attractive Solution*, *JHEP* **07** (2018) 151 [arXiv:1806.04677] [INSPIRE].

[69] D.G. Figueroa, M. Hindmarsh, J. Lizarraga and J. Urrestilla, *Irreducible background of gravitational waves from a cosmic defect network: update and comparison of numerical techniques*, *Phys. Rev. D* **102** (2020) 103516 [arXiv:2007.03337] [INSPIRE].

[70] M. Gorghetto, E. Hardy and H. Nicolaescu, *Observing invisible axions with gravitational waves*, *JCAP* **06** (2021) 034 [arXiv:2101.11007] [INSPIRE].

[71] C.-F. Chang and Y. Cui, *Gravitational waves from global cosmic strings and cosmic archaeology*, *JHEP* **03** (2022) 114 [arXiv:2106.09746] [INSPIRE].

[72] J.T. Giblin and J.B. Mertens, *Gravitional radiation from first-order phase transitions in the presence of a fluid*, *Phys. Rev. D* **90** (2014) 023532 [arXiv:1405.4005] [INSPIRE].

[73] M. Hindmarsh, S.J. Huber, K. Rummukainen and D.J. Weir, *Gravitational waves from the sound of a first order phase transition*, *Phys. Rev. Lett.* **112** (2014) 041301 [arXiv:1304.2433] [INSPIRE].

JHEP10(2023)158

[74] D. Cutting, M. Hindmarsh and D.J. Weir, *Vorticity, kinetic energy, and suppressed gravitational wave production in strong first order phase transitions*, *Phys. Rev. Lett.* **125** (2020) 021302 [arXiv:1906.00480] [INSPIRE].

[75] M. Hindmarsh, S.J. Huber, K. Rummukainen and D.J. Weir, *Numerical simulations of acoustically generated gravitational waves at a first order phase transition*, *Phys. Rev. D* **92** (2015) 123009 [arXiv:1504.03291] [INSPIRE].

[76] M. Hindmarsh, S.J. Huber, K. Rummukainen and D.J. Weir, *Shape of the acoustic gravitational wave power spectrum from a first order phase transition*, *Phys. Rev. D* **96** (2017) 103520 [*Erratum ibid.* **101** (2020) 089902] [arXiv:1704.05871] [INSPIRE].

[77] D. Cutting, M. Hindmarsh and D.J. Weir, *Gravitational waves from vacuum first-order phase transitions: from the envelope to the lattice*, *Phys. Rev. D* **97** (2018) 123513 [arXiv:1802.05712] [INSPIRE].

[78] D. Cutting, E.G. Escartin, M. Hindmarsh and D.J. Weir, *Gravitational waves from vacuum first order phase transitions II: from thin to thick walls*, *Phys. Rev. D* **103** (2021) 023531 [arXiv:2005.13537] [INSPIRE].

[79] A. Roper Pol et al., *Numerical simulations of gravitational waves from early-universe turbulence*, *Phys. Rev. D* **102** (2020) 083512 [arXiv:1903.08585] [INSPIRE].

[80] S. Blasi and A. Mariotti, *Domain Walls Seeding the Electroweak Phase Transition*, *Phys. Rev. Lett.* **129** (2022) 261303 [arXiv:2203.16450] [INSPIRE].

[81] D. Curtin, P. Meade and C.-T. Yu, *Testing Electroweak Baryogenesis with Future Colliders*, *JHEP* **11** (2014) 127 [arXiv:1409.0005] [INSPIRE].

[82] L. Bian, Y. Wu and K.-P. Xie, *Electroweak phase transition with composite Higgs models: calculability, gravitational waves and collider searches*, *JHEP* **12** (2019) 028 [arXiv:1909.02014] [INSPIRE].

[83] P. Huang, A.J. Long and L.-T. Wang, *Probing the Electroweak Phase Transition with Higgs Factories and Gravitational Waves*, *Phys. Rev. D* **94** (2016) 075008 [arXiv:1608.06619] [INSPIRE].

[84] D.J.H. Chung, A.J. Long and L.-T. Wang, *125 GeV Higgs boson and electroweak phase transition model classes*, *Phys. Rev. D* **87** (2013) 023509 [arXiv:1209.1819] [INSPIRE].

[85] P.M. Schicho, T.V.I. Tenkanen and J. Österman, *Robust approach to thermal resummation: Standard Model meets a singlet*, *JHEP* **06** (2021) 130 [arXiv:2102.11145] [INSPIRE].

[86] L. Niemi, P. Schicho and T.V.I. Tenkanen, *Singlet-assisted electroweak phase transition at two loops*, *Phys. Rev. D* **103** (2021) 115035 [arXiv:2103.07467] [INSPIRE].

[87] T. Gorda et al., *Three-dimensional effective theories for the two Higgs doublet model at high temperature*, *JHEP* **02** (2019) 081 [arXiv:1802.05056] [INSPIRE].

[88] K. Kainulainen et al., *On the validity of perturbative studies of the electroweak phase transition in the Two Higgs Doublet model*, *JHEP* **06** (2019) 075 [arXiv:1904.01329] [INSPIRE].

[89] D. Croon et al., *Theoretical uncertainties for cosmological first-order phase transitions*, *JHEP* **04** (2021) 055 [arXiv:2009.10080] [INSPIRE].

[90] P. Schicho, T.V.I. Tenkanen and G. White, *Combining thermal resummation and gauge invariance for electroweak phase transition*, *JHEP* **11** (2022) 047 [arXiv:2203.04284] [INSPIRE].

JHEP10(2023)158

[91] J. Borrill, T.W.B. Kibble, T. Vachaspati and A. Vilenkin, *Defect production in slow first order phase transitions*, *Phys. Rev. D* **52** (1995) 1934 [hep-ph/9503223] [INSPIRE].

[92] S. Digal, S. Sengupta and A.M. Srivastava, *Vortex-antivortex pair production in a first order phase transition*, *Phys. Rev. D* **56** (1997) 2035 [hep-ph/9705246] [INSPIRE].

[93] E.J. Copeland and P.M. Saffin, *Bubble collisions in Abelian gauge theories and the geodesic rule*, *Phys. Rev. D* **54** (1996) 6088 [hep-ph/9604231] [INSPIRE].

[94] S. Digal, S. Sengupta and A.M. Srivastava, *Simulation of vortex-antivortex pair production in a phase transition with explicit symmetry breaking*, *Phys. Rev. D* **58** (1998) 103510 [hep-ph/9707221] [INSPIRE].

[95] A. Ferrera and A. Melfo, *Bubble collisions and defect formation in a damping environment*, *Phys. Rev. D* **53** (1996) 6852 [hep-ph/9512290] [INSPIRE].

[96] A. Ferrera, *How does the geodesic rule really work for global symmetry breaking first order phase transitions?*, *Phys. Rev. D* **59** (1999) 123503 [hep-ph/9811269] [INSPIRE].

[97] A. Ferrera, *Defect formation in first order phase transitions with damping*, *Phys. Rev. D* **57** (1998) 7130 [hep-ph/9612487] [INSPIRE].

[98] E.J. Copeland, P.M. Saffin and O. Tornkvist, *Phase equilibration and magnetic field generation in* U(1) *bubble collisions*, *Phys. Rev. D* **61** (2000) 105005 [hep-ph/9907437] [INSPIRE].

[99] A.-C. Davis and M. Lilley, *Cosmological consequences of slow moving bubbles in first order phase transitions*, *Phys. Rev. D* **61** (2000) 043502 [hep-ph/9908398] [INSPIRE].

[100] M. Lilley and A. Ferrera, *Defect formation rates in cosmological first order phase transitions*, *Phys. Rev. D* **64** (2001) 023520 [hep-ph/0102035] [INSPIRE].

[101] J. Liu et al., *Primordial black hole production during first-order phase transitions*, *Phys. Rev. D* **105** (2022) L021303 [arXiv:2106.05637] [INSPIRE].

[102] J. Liu et al., *Constraining First-Order Phase Transitions with Curvature Perturbations*, *Phys. Rev. Lett.* **130** (2023) 051001 [arXiv:2208.14086] [INSPIRE].

[103] A. Masoumi, K.D. Olum and J.M. Wachter, *Approximating tunneling rates in multi-dimensional field spaces*, *JCAP* **10** (2017) 022 [*Erratum ibid.* **05** (2023) E01] [arXiv:1702.00356] [INSPIRE].

[104] V. Guada, M. Nemevšek and M. Pintar, *FindBounce: Package for multi-field bounce actions*, *Comput. Phys. Commun.* **256** (2020) 107480 [arXiv:2002.00881] [INSPIRE].

[105] J.M. Cline and K. Kainulainen, *Electroweak baryogenesis and dark matter from a singlet Higgs*, *JCAP* **01** (2013) 012 [arXiv:1210.4196] [INSPIRE].

[106] V. Vaskonen, *Electroweak baryogenesis and gravitational waves from a real scalar singlet*, *Phys. Rev. D* **95** (2017) 123515 [arXiv:1611.02073] [INSPIRE].

[107] T. Konstandin, *Gravitational radiation from a bulk flow model*, *JCAP* **03** (2018) 047 [arXiv:1712.06869] [INSPIRE].

[108] J. Ellis, M. Lewicki and V. Vaskonen, *Updated predictions for gravitational waves produced in a strongly supercooled phase transition*, *JCAP* **11** (2020) 020 [arXiv:2007.15586] [INSPIRE].

[109] M. Lewicki and V. Vaskonen, *Gravitational waves from colliding vacuum bubbles in gauge theories*, *Eur. Phys. J. C* **81** (2021) 437 [*Erratum ibid.* **81** (2021) 1077] [arXiv:2012.07826] [INSPIRE].

JHEP10(2023)158

[110] J. Garcia-Bellido, D.G. Figueroa and A. Sastre, *A Gravitational Wave Background from Reheating after Hybrid Inflation*, *Phys. Rev. D* **77** (2008) 043517 [arXiv:0707.0839] [INSPIRE].

[111] P. Adshead, J.T. Giblin, M. Pieroni and Z.J. Weiner, *Constraining axion inflation with gravitational waves from preheating*, *Phys. Rev. D* **101** (2020) 083534 [arXiv:1909.12842] [INSPIRE].

[112] M. Hindmarsh and M. Hijazi, *Gravitational waves from first order cosmological phase transitions in the Sound Shell Model*, *JCAP* **12** (2019) 062 [arXiv:1909.10040] [INSPIRE].

[113] S.J. Huber and T. Konstandin, *Gravitational Wave Production by Collisions: More Bubbles*, *JCAP* **09** (2008) 022 [arXiv:0806.1828] [INSPIRE].

[114] M. Kamionkowski, A. Kosowsky and M.S. Turner, *Gravitational radiation from first order phase transitions*, *Phys. Rev. D* **49** (1994) 2837 [astro-ph/9310044] [INSPIRE].

[115] R.-G. Cai, S. Pi and M. Sasaki, *Universal infrared scaling of gravitational wave background spectra*, *Phys. Rev. D* **102** (2020) 083528 [arXiv:1909.13728] [INSPIRE].

[116] C. Caprini, R. Durrer and G. Servant, *The stochastic gravitational wave background from turbulence and magnetic fields generated by a first-order phase transition*, *JCAP* **12** (2009) 024 [arXiv:0909.0622] [INSPIRE].

[117] A. Saurabh, T. Vachaspati and L. Pogosian, *Decay of Cosmic Global String Loops*, *Phys. Rev. D* **101** (2020) 083522 [arXiv:2001.01030] [INSPIRE].

[118] A. Vilenkin and A.E. Everett, *Cosmic Strings and Domain Walls in Models with Goldstone and PseudoGoldstone Bosons*, *Phys. Rev. Lett.* **48** (1982) 1867 [INSPIRE].

JHEP10(2023)158